Anomalous diffusion of tracer in convection rolls

W. Young
Scripps Institution of Oceanography, La Jolla, California 92093
A. Pumir[a] and Y. Pomeau
Ecole Normale Supérieure, 24 Rue Lhomond 75231, Paris, France

(Received 2 May 1988; accepted 1 November 1988)

The dispersion of a passive tracer in a two-dimensional, spatially periodic stationary flow, such as convection rolls, is studied in the large Peclet number limit. In the case where injection, at time $t = 0$, is localized in one roll, two regimes exist. First, there is an anomalous diffusion regime in which the number of invaded rolls grows like $t^{1/3}$. This regime is due to the presence of separatrices between rolls that induce trapping of tracer within each roll. At a later time, when $t \gg T_d$ (the diffusion time within a roll), the usual diffusion regime is recovered, yet with an effective diffusive coefficient κ_{eff} that is greater than the molecular diffusivity κ by a factor proportional to the square root of the Peclet number.

I. INTRODUCTION

This paper considers the dispersion of a passive scalar ("tracer") in a periodic array of convection cells. The complete evolution of the concentration θ is determined by the advection–diffusion equation

$$\partial_t \theta + J(\varphi,\theta) = \kappa \nabla^2 \theta, \tag{1}$$

where φ is the streamfunction from which the incompressible, two-dimensional steady velocity field

$$(u,v) = (-\partial_y \varphi, \partial_x \varphi) \tag{2}$$

is obtained. The molecular diffusivity κ is assumed to be very small or, more precisely, the Peclet number

$$P_e \equiv \varphi_{\max}/\kappa \tag{3}$$

is large. The boundary conditions on the velocity field are "no slip," i.e., $u = 0$ on $y = 0$ and L_y in Fig. 1. By convention, the streamfunction is zero on the separatrices and on the walls.

Our goal here is a simplified or averaged description of the evolution of an initially compact distribution of tracer. The basic variable is the averaged concentration

$$g_n(t) \equiv A^{-1} \int \theta \, dA_n, \tag{4}$$

where the integral above is over the area occupied by the nth cell and $A = L_x L_y$ is the area of a cell. Our notation is introduced in Fig. 1. Unlike recent work on the same[1,2] or similar problems,[3] we discuss the dispersion on intermediate time scales,

$$A/\varphi_{\max} \ll t \ll A/\kappa, \tag{5}$$

before the tracer has reached the center of recently invaded cells. Even though the time is much less than the intracellular diffusion time A/κ, a substantial lateral spread of the tracer can occur and, in fact, the number of cells invaded increases as $t^{1/3}$.[4] At times much larger than A/κ, this anomalous diffusion is replaced by the familiar Fickian result, so that the number of invaded cells increases at $t^{1/2}$. In this long time limit, our formalism reduces to a conventional diffusion equation and is identical to that of earlier investigators.[1,2]

On intermediate time scales, such as in (5), the dispersion is complicated by the nonuniform distribution of tracer within a cell. Thus transfer between cells is proportional to *peripheral* concentration differences, but these are obviously not related to the *average* concentration defined in Eq. (4). It turns out that

$$f_n \equiv \frac{\oint \theta q \, dl}{\oint q \, dl}, \tag{6a}$$

$$q \equiv (u^2 + v^2)^{1/2}, \tag{6b}$$

where the line integrals above are around the perimeter of the nth cell, are a useful measure of the peripheral concentration. In fact, intercellular transports are proportional to differences in f_n and conservation of tracer is just

$$\frac{dg_n}{dt} = s(f_{n+1} - 2f_n + f_{n-1}), \tag{7}$$

where s^{-1} is a time scale found below. A second relation between f_n and g_n is obtained by considering the spread of tracer within a single cell. This leads to

$$g_n(t) \equiv \int_0^t K(t-\tau) f_n(\tau) d\tau, \tag{8}$$

and together, (7) and (8) constitute the averaged description of tracer dispersion. Exact expressions for the kernel K in (8) are not easily found, but on intermediate time scales it has the form

$$K(\tau) \propto \tau^{-2/3}, \tag{9}$$

while at times much greater than A/κ,

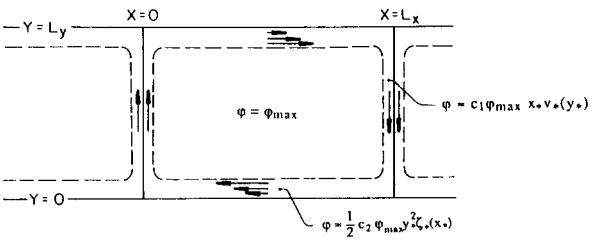

FIG. 1. Definition sketch showing the local behavior of the streamfunction at the edge of a cell. Here, c_1 and c_2 are dimensionless constants and ζ_* and v_* are dimensionless functions with dimensionless arguments.

[a] S.Ph.T., C.E.N., Saclay 91191, Gif sur Yvette, France.

 0899-8213/89/030462-08$01.90

$$K(\tau) \propto e^{-\mu\tau}, \tag{10}$$

where μ^{-1} is a time of order A/κ. The anomalous dispersion referred to earlier results from the slow decay in (9), and the Fickian regime is reached when the structure of the kernel changes to that in (10).

In Sec. II we derive (8) and discuss the physical interpretation of the kernel $K(\tau)$. In Sec. III we obtain (7), and then in Sec. IV we discuss the solution of the system (7) and (8), emphasizing the anomalous diffusion regime.

II. THE INTRACELLULAR DIFFUSION PROBLEM

In this section we consider the details of how tracer contaminates an initially unpolluted cell. We suppose, for the moment, that the distribution of tracer on the edge of the cell is known as a function of time and arclength. Our goal is the relation (8) that connects the total amount of tracer within the cell to a history convolution of a velocity-weighted peripheral average. Thus we examine a particular cell and solve (1), assuming that P_e in (3) is very large. The initial condition is

$$\theta(x, y, 0) = 0, \tag{11}$$

and we suppose that the boundary distribution of θ is a known function of arclength l and time t, denoted by χ:

$$\theta(\partial A, t) = \chi(l, t), \tag{12}$$

where ∂A is the boundary of a cell.

This problem can be solved using the technique in Rhines and Young,[5] and in Fowler.[6] A brief summary is given in Appendix A. The essential result there is that when $P_e \gg 1$, the tracer distribution in the *interior* is uniform on streamlines, i.e.,

$$\theta(x, y, t) \simeq \bar{\theta}(\varphi, t) \equiv \frac{\oint \theta(dl/q)}{\oint (dl/q)}, \tag{13}$$

where the line integrals are around streamlines. Using averaging techniques, (1) is reduced to

$$T(\varphi)\partial_t \bar{\theta} = \kappa\, \partial_\varphi [C(\varphi)\partial_\varphi \bar{\theta}], \tag{14}$$

where

$$T(\varphi) = \oint \frac{dl}{q} \tag{15}$$

is the transit time around a streamline and

$$C(\varphi) = \oint q\, dl \tag{16}$$

is the absolute value of the circulation around a streamline.

Clearly the formulation above fails near the boundary of the cell where (12) shows that there are generally substantial variations in tracer concentration imposed along a streamline. Instead, there is a boundary layer at the edge of the cell in which the externally imposed distribution in (12) is transformed into an "effective boundary condition" for (14). Fortunately, a detailed analysis of the boundary layer can be avoided and instead one can show that (see Appendix A)

$$\bar{\theta}(0, t) = \frac{\oint \chi q\, dl}{\oint q\, dl} \tag{17}$$

is the effective boundary condition for (14). It is notable that in the interior of the cell, the appropriate streamline average is a time average [see (13)], while at the boundary of the cell the velocity-weighted average above is appropriate. The physical explanation is that large velocities mean that streamlines are close together and boundary values of θ in these regions can diffuse across a greater range of streamlines. Thus boundary values juxtaposed with large velocities are most effectively transferred into the interior of the cell.

There is one final transformation that is useful, this being the use of the area inside a streamline $a(\varphi)$ as an independent variable. As explained in Rhines and Young,[5]

$$\frac{da}{d\varphi} = \oint \frac{dl}{q} = T, \tag{18}$$

so that in terms of a, (14) becomes

$$\partial_t \bar{\theta} = \partial_a D\, \partial_a \bar{\theta}, \tag{19a}$$

$$D(a) \equiv \kappa C(a) T(a), \tag{19b}$$

with an initial condition in (11) and a boundary condition at $a = A$:

$$\bar{\theta}(A, t) = \frac{\oint \chi q\, dl}{\oint q\, dl} \equiv f(t). \tag{20}$$

Before solving the diffusion equation in (19), we must calculate $D(a)$. Even for simple model streamfunctions this is tedious. However, if, as in Fig. 1, the boundaries at $y = 0$ and L_y are no slip, then a local analysis shows that $D(a)$ has the form

$$D(a) \approx \Delta(1 - a/A)^{-1}, \quad \text{if } a \approx A, \tag{21a}$$

$$D(a) \approx \Gamma a, \quad \text{if } a \ll A. \tag{21b}$$

Explicit expressions for Δ in (21a) are given in Appendix B. The important point is that $D(a)$ is singular at the outer streamline, because $T(a)$ in (19b) becomes infinite as φ approaches zero, or equivalently, a approaches A. This is a result of the no-slip boundary condition on the walls at $y = 0$ and L_y.

Now, because (19) and (20) are linear, the total amount of tracer in the cell

$$Ag \equiv \int \theta\, dA \approx \int_0^A \theta(a, t)\, da$$

must be related to the boundary condition on (20) by an expression of the form

$$g(t) = \int_0^t K(t - \tau) f(\tau)\, d\tau, \tag{22}$$

and in the early stages of the process, when most of the tracer is still in regions where (21a) is accurate, we can find $K(\tau)$.

Begin by introducing the Laplace transform

$$\tilde{\theta} \equiv \int_0^\infty e^{-pt} \bar{\theta}\, dt, \tag{23}$$

and using

$$z \equiv (A - a)/A \tag{24}$$

as an independent variable. With (21a), the diffusion equation (19a) becomes

$$p\tilde{\theta} = \lambda\, \partial_z z^{-1}\, \partial_z \tilde{\theta}, \tag{25}$$

where

$$\lambda \equiv \Delta/A^2 \propto \kappa/L_x^2 \tag{26}$$

is an inverse time scale. The solution of (25) is

$$\tilde{\theta} = \tilde{f}(p) A_i'[(p/\lambda)^{1/3} z]/A_i'(0), \tag{27}$$

where A_i' is the derivative of the Airy function. We can immediately calculate

$$\tilde{g} \approx A^{-1} \int_0^\infty da\, \tilde{\theta}, \tag{28a}$$

$$= (\Gamma(\tfrac{1}{3})/3^{1/3}\Gamma(\tfrac{2}{3}))(\lambda/p)^{1/3}\tilde{f}(p), \tag{28b}$$

and now, because the Laplace transform of t^α is $\Gamma(1+\alpha)p^{-\alpha-1}$, the convolution theorem gives

$$g = \left(3^{1/3}\Gamma\left(\frac{2}{3}\right)\right)^{-1} \lambda^{1/3} \int_0^t (t-\tau)^{-2/3} f(\tau)\, d\tau, \tag{29}$$

which is the desired relation between the amount of tracer within a cell and the boundary averaged concentration. Introduction of the Riemann–Liouville fractional integral

$$I^v f \equiv \Gamma(v)^{-1} \int_0^t (t-\tau)^{v-1} f(\tau)\, d\tau \tag{30}$$

puts (29) in a slightly more compact form,

$$g = (\Gamma(\tfrac{1}{3})/\Gamma(\tfrac{2}{3})3^{1/3})\lambda^{1/3} I^{1/3} f, \tag{31}$$

and emphasizes the connection of the present problem with that in Ref. 7.

III. INTERCELLULAR TRANSFERS

The flux of tracer between two adjacent cells, say n and $n+1$, is

$$F = -\kappa \int_0^{L_y} \theta_x\, dy. \tag{32}$$

This can be calculated explicitly using boundary layer theory. Perhaps the simplest illustration of this calculation is obtained by supposing that in Fig. 2 the concentration along the section AA', entering the boundary layer, is uniform and equal to $f_{n+1}(t)$. This is actually the case if L_x is long enough to ensure that the tracer profile leaving DD'' is well mixed by the time it reaches AA'. Because of the much greater tracer content of the cell interior, this well-mixed concentration will equal the concentration at the outer edge of the interior. Likewise, in cell n, the profile at AA'' is uniform and equal to $f_n(t)$. Precise estimates of how large L_x must be to ensure this simple, discontinuous entry profile for the boundary layer are contained in Appendix C. In that same Appendix we discuss the complementary case where L_x is so short that the profile at DD'' is transported without significant change to AA'. Using scale analysis, we conclude that the transition between these two complementary limits takes place when $L_x/L_y = O(P_e^{1/7})$.

Within the boundary layer the dominant balance in the advection–diffusion equation is (A4), and the solution of this is

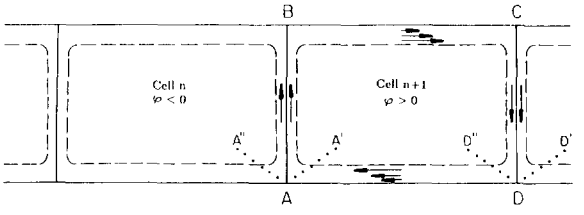

FIG. 2. A definition of the notation used to calculate the flux of tracer between cell n and cell $n+1$. There are boundary layers along the separatrices AB and CD.

$$\theta = \tfrac{1}{2}(f_{n+1} + f_n) + \tfrac{1}{2}(f_{n+1} - f_n)\,\mathrm{erf}(\eta), \tag{33a}$$

$$\eta \equiv \varphi/\sqrt{4\kappa s}, \tag{33b}$$

where $s = 0$ is the section $A''AA'$ at the mouth of the boundary layer, and we have supposed that $\varphi > 0$ in cell $n+1$ and $\varphi < 0$ in cell n. Using (33) and the definition of s in (A3), the flux in (32) is

$$F = -\gamma\sqrt{\phi_{\max}\kappa L_y/L_x}\,(f_{n+1} - f_n), \tag{34a}$$

$$\gamma \equiv \sqrt{\frac{c_1}{\pi}\int_0^1 v_*\, dy_*}\,, \tag{34b}$$

where the dimensionless variables c_1 and v_* are defined in Fig. 1. In Shraiman[2] this flux is evaluated in the complementary limit where L_x is so short that no mixing occurs as tracer passes along the horizontal portion of the boundary. The result is identical to (34a) except that

$$\gamma \equiv 1.521 \sqrt{\frac{1}{\pi}\int_0^1 v_*\, dy_*}\,. \tag{35}$$

To summarize, the flux between cells is proportional to peripheral concentration differences, $f_{n+1} - f_n$. It follows that conservation of tracer is given by (7), with

$$s = \gamma\sqrt{\kappa\varphi_{\max}/L_x^3 L_y}\,. \tag{36}$$

Finally, if the changes in f_n between adjacent cells are small, then (7) becomes

$$\partial_t g = \kappa_{\text{eff}}\, \partial_x^2 f, \tag{37}$$

where $x = nL_x$ is now a slow spatial scale and

$$\kappa_{\text{eff}} = sL_x^2,$$

$$= \gamma\sqrt{\kappa\phi_{\max} L_x/L_y} \tag{38}$$

is an effective diffusivity. Equation (37), together with

$$g(x,t) = \int_0^t K(t-\tau) f(x,\tau)\, d\tau, \tag{39}$$

is the final, averaged description of the evolution of the tracer.

IV. ANOMALOUS DIFFUSION

In this section, we solve explicitly the two coupled equations [(6) and (8)] for the two unknown functions f and g. We show that when the kernel has the form in (30), these

equations indeed lead to an anomalous diffusion regime in which space and time are related by $x \approx t^{\alpha}$, with $\alpha \equiv (1-\nu)/2$. In particular, the Green's function for these equations is computed and shown to depend on the similarity variable $\eta \propto |x|/t^{\alpha}$. With no-slip boundary conditions we have shown in (29) that $\nu = \frac{1}{3}$, and so $\alpha = \frac{1}{3}$. Consequently the number of convection cells invaded by tracer grows as $t^{1/3}$. It has also been argued that at later times (30) is invalid. Physically, this occurs when tracer has enough time to invade the whole roll and the kernel in (30) has to be replaced by an exponentially decaying function of time. The case of a modified kernel,

$$K(\tau) = \Gamma(\nu)^{-1}\tau^{\nu-1}\exp(-\mu\tau)$$

(with $\nu = \frac{1}{3}$) that behaves like $t^{-2/3}$ for short time and like $e^{-\mu t}$ for long time, is also studied. It is found that the anomalous diffusion regime is replaced by normal diffusive behavior at later times. The crossover regime is studied in some detail.

Although the problem of interest in this paper corresponds to $\nu = \frac{1}{3}$, other situations with different exponents can be encountered, and so it is of interest to retain ν as a parameter. In particular, it is shown in Ref. 7 that similar equations describe situations where dispersion in the x direction is interrupted by pauses or stops of random duration. The kernel in (39) is related to the probability distribution of pause duration. In the present problem, the pauses are produced by tracer molecules wandering in the interior of convection cells. It is not until their random walk across interior streamlines returns them to the edge of the cell that they can hop into an adjacent cell and so disperse macroscopically.

In the following, we work with rescaled versions of (31) and (37), formed by introducing the dimensionless time and space variables, respectively,

$$T = \lambda t\,[\Gamma^3(\tfrac{1}{3})/3\Gamma^3(\tfrac{2}{3})],$$

$$X = x(\lambda/\kappa_{\text{eff}})^{1/2}[\Gamma^3(\tfrac{1}{3})/3\Gamma^3(\tfrac{2}{3})]^{1/2}.$$

With this notation, Eqs. (37) and (31) read

$$\partial_T g = \partial_{XX} f, \tag{40a}$$

$$g = I^{\nu} f, \tag{40b}$$

where

$$I^{\nu} f = \frac{1}{\Gamma(\nu)}\int_0^T (T-\tau)^{\nu-1} f(\tau)\,d\tau. \tag{41}$$

We are interested in determining the Green's function for this problem and so we specify the initial condition $g(X,0) = \delta(X)$. In physical terms, this corresponds to a roll filled with tracer at $T = 0$, all the others being uncontaminated. Although the case of interest here is $\nu = \frac{1}{3}$, we will solve the problem with an arbitrary ν (subject to the restriction $0 < \nu < 1$). In the more realistic case, with the exponential damping in the kernel, (41) has to be replaced by

$$g = \frac{1}{\Gamma(\frac{1}{3})}\int_0^T (T-\tau)^{-2/3} e^{-\mu(T-\tau)} f(\tau)\,d\tau, \tag{42}$$

where μ is a number of order 1. In our units, the damping becomes effective when $T \approx 1$, that is, when tracer has enough time to completely invade a roll.

We start with the case $\mu = 0$. In order to solve Eqs. (40) we use the Laplace transform,

$$\tilde{g}(p) = \int_0^{+\infty} e^{-pT} g(T)\,dT. \tag{43}$$

The Laplace transform of $I^{\nu} f$ is simply the product of the Laplace transform of f by $p^{-\nu}$. After simple manipulations, Eqs. (41) and (42) become

$$\tilde{g}(p) = p^{-\nu}\tilde{f}, \tag{44}$$

$$\partial_{XX}\tilde{f} - p^{1-\nu}\tilde{f} = -\delta(X). \tag{45}$$

The solution of these equations can be readily obtained:

$$\tilde{f} = (\tfrac{1}{2})p^{(\nu-1)/2}\exp(-p^{-(\nu-1)/2}\xi), \tag{46}$$

$$\tilde{g} = (\tfrac{1}{2})p^{-(\nu+1)/2}\exp(-p^{-(\nu-1)/2}\xi), \tag{47}$$

where ξ denotes the absolute value of X. In order to evaluate the original functions, one has to perform the inverse Laplace transform of these two functions. The result is

$$f(\xi,T) = \frac{1}{4i\pi}\int_{-\infty}^{+\infty} dp\, p^{(\nu-1)/2} e^{pT - \xi p^{\alpha}}, \tag{48a}$$

$$f(\xi,T) = \frac{1}{4i\pi}\int_{-\infty}^{+\infty} dp\, p^{(\nu-1)/2} e^{pT\xi p^{\alpha}}, \tag{48b}$$

where $\alpha = (1-\nu)/2$. It is sometimes possible to express these integrals in simpler terms. In fact, when $\nu = \frac{1}{3}$ and $\alpha = \frac{1}{3}$, one can show that (48b) reduces to

$$g = \tfrac{1}{2}(9/T)^{1/3} A_i[\xi/(3T)^{1/3}],$$

where $A_i(z)$ is the Airy function. This Green's function is plotted as the solid curve in Fig. 3. However, for the general case, it is more fruitful to use asymptotic methods such as the saddle point method.[8] It is convenient to introduce first the change of variables:

$$p = (\xi/T)^{1/(1-\alpha)} u.$$

One then obtains

$$f(\xi,T) = \frac{1}{4i\pi}\left(\frac{\xi}{T}\right)\int_{-\infty}^{+\infty} du\, u^{-\alpha} e^{\omega(u-u^{\alpha})}, \tag{48a'}$$

$$g(\xi,T) = \frac{1}{4i\pi}\left(\frac{\xi}{T}\right)[\alpha/(1-\alpha)]\int_{-\infty}^{+\infty} du\, u^{\alpha-1} e^{\omega(u-u^{\alpha})}, \tag{48b'}$$

with $\omega \equiv (\xi/T^{\alpha})^{1/(1-\alpha)}$. In this form, it is obvious that the functions f and g depend on the similarity variable ω, with an algebraic prefactor. The integrand that defines f or g is of the form $h(u)\exp(\omega q(u))$, where $q(u) = u - u^{\alpha}$. At large values of ω, the argument of the exponential has wild variations in u. Therefore it is appropriate to use the saddle point method in this limit. The saddle point is defined by the condition

$$q'(u_s) = 0 \quad \text{or} \quad u_s = \alpha^{1/(1-\alpha)}. \tag{49}$$

The saddle point is thus real and positive. The value of q at u_s is

$$q_s = (1-\alpha^{-1})u_s. \tag{50}$$

In order to completely evaluate the integral, it is also neces-

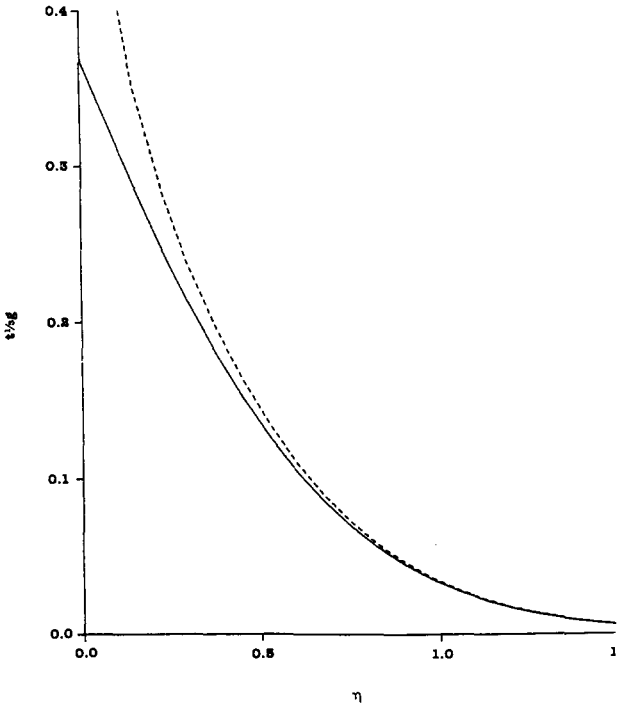

FIG. 3. The rescaled Green's function $t^{1/2}(g(\eta))$. The solid curve is the exact expression, $(3^{2/3}/2)A_i(3^{2/3}\eta)$, and the dashed curve is the asymptotic expansion in (53).

sary to compute the second derivative of q at the saddle point. The result is

$$q_s'' = (1-\alpha)/u_s. \tag{51}$$

Using standard results (8), one obtains the asymptotic expression

$$g \sim [T^{-\alpha}/2\sqrt{\pi(1+\nu)}]\eta^{(1-2\alpha)/2(\alpha-1)} \times \exp[(1-\alpha^{-1})\eta^{1/(1-\alpha)}], \tag{52a}$$

$$\eta \equiv \alpha\xi/T^{\alpha} = (\omega u_s)^{1-\alpha}. \tag{52b}$$

A familiar limit is $\nu \to 0$ and $\alpha \to \frac{1}{2}$, so that (52a) becomes the Gaussian

$$g \sim (1/2\sqrt{\pi T})\exp(-X^2/4T),$$

which is actually an exact expression for the Green's function. In this case the kernel decays so quickly that there is no anomalous regime. The complementary limit is $\nu \to 1$ and $\alpha \to 0$, so that

$$g \sim (T^{-\alpha}/2\sqrt{2\pi})(T^{\alpha}/\alpha\xi)^{1/2} e^{-|X|/T^{\alpha}}.$$

It has to be noted that the limit $\alpha \to 0$ is a little bit more complicated. In fact, the limit formula obtained above is not uniformly valid when $\alpha \to 0$. The reason is that at a fixed value of ω, when α decreases, the variations of the term ωu^{α} become negligible compared to the variations of the algebraic prefactor in the integral (48b'). It can be shown that the saddle point method is correct as long as $(\alpha\xi/T^{\alpha}) \gg 1$. When this is not the case, a better approximation of the integral is obtained by holding the factor $\exp(-\omega u^{\alpha})$ fixed and equal to $\exp(-\omega)$, and computing the remaining integral in u. The result is

$$g \sim (T^{-\alpha}/2)e^{-|X|/T^{\alpha}}.$$

This result can be guessed in a simpler way. When $\nu = 1$, the operator $I^{\nu}f$ is the operator of integration and Eqs. (40a) and (40b) can be integrated in a straightforward manner.

In between these two limits is the case $\nu = \frac{1}{2}$, $\alpha = \frac{1}{4}$, where (52) reproduces the asymptotic expansion found in Ref. 7, and the case most relevant to dispersion in convection rolls, viz., $\nu = \alpha = \frac{1}{3}$, for which

$$g \sim (T^{-1/3}/4)\sqrt{(3/\pi)}\eta^{-1/4}\exp(-2\eta^{3/2}). \tag{53}$$

The similarity variable, $\eta = |X|/3T^{1/3}$, shows that the intuitive argument in Guyon *et al.*[4] and Pomeau *et al.*[4] correctly anticipates the anomalous power law. The result in (53) can also be found from the previous analytic expression using the standard asymptotic expansion of the Airy function. Figure 3 compares the asymptotic expression in (53) with the exact result.

We now turn to the problem of the transition between the short time, anomalous diffusion behavior and the long time, purely diffusive behavior. The model kernel we choose to treat this problem, $K(\tau) = \Gamma(\nu)^{-1}\tau^{\nu-1}\exp(-\mu\tau)$, behaves like the kernel we just considered at short times, and decays exponentially for times much larger than μ^{-1}.

There is one consistency condition that any model kernel must satisfy. This is

$$\int_0^{\infty} K(\tau)d\tau = 1,$$

so that if $f(t)$ is held constant, then $g(t)$ will eventually equilibrate at this same constant value. With the model kernel, $K(\tau) = \Gamma(\frac{1}{3})^{-1}\tau^{-2/3}\exp(-\mu\tau)$. This consistency condition implies $\mu = 1$. Nonetheless, it is convenient to retain the parameter μ in the following calculation. More complicated model kernels might have an exponential decay with some other e-folding time and the results below apply to this case as well. Again, we treat the two coupled equations, (40a) and

$$g(T) = \int_0^T K(T-\tau)f(\tau)d\tau, \tag{54}$$

using the Laplace transform. It turns out that the Laplace transform of the modified kernel is particularly simple and well suited for an analysis of our problem. Explicitly, the Laplace transform of (54) is

$$\tilde{g}(p) = (p+\mu)^{-\nu}\tilde{f}(p). \tag{55}$$

Inserting this into the Laplace transform of (40), one obtains [instead of (45)]

$$\partial_{XX}\tilde{f} - p(p+\mu)^{-\nu}\tilde{f} = -\delta(X). \tag{56}$$

The solution of this equation, as well as an explicit expression for the Laplace transform of g, are readily obtained:

$$\tilde{f}(p,X) = \tfrac{1}{2}p^{-1/2}(p+\mu)^{\nu/2}\exp(-p^{1/2}(p+\mu)^{-\nu/2}\xi), \tag{57}$$

$$\tilde{g}(p,X) = \tfrac{1}{2} p^{-1/2}(p+\mu)^{-\nu/2} \exp(-p^{1/2}(p+\mu)^{-\nu/2}\xi). \tag{58}$$

The inverse of the Laplace transform is found by integrating these expressions along a path parallel to the imaginary axis in the p plane:

$$f(\xi,T) = \frac{1}{4i\pi}\int_{-\infty}^{+\infty} dp\, p^{-1/2}(p+\mu)^{\nu/2} \times \exp(pT - \xi^{1/2}p^{1/2}(p+1)^{-\nu/2}), \tag{59}$$

$$g(\xi,T) = \frac{1}{4i\pi}\int_{-\infty}^{+\infty} dp\, p^{-1/2}(p+\mu)^{-\nu/2} \times \exp(pT - \xi p^{1/2}(p+\mu)^{-\nu/2}). \tag{60}$$

As in the previous case, it is convenient to use the saddle point method in order to evaluate the behavior of the functions f and g. Again, we change variables: $p = u(\xi/t^{\alpha})^{1/(1-\alpha)}$. The integrals (59) and (60) become

$$f(\xi,T) = \frac{1}{4i\pi}\left(\frac{\xi}{T}\right)\int_{-\infty}^{+\infty} du\, u^{-1/2}(u+\lambda)^{\nu/2} \times \exp[\omega(u - u^{1/2}(u+\lambda)^{-\nu/2})], \tag{59'}$$

$$g(\xi,T) = \frac{1}{4i\pi}\left(\frac{\xi}{T}\right)^{\alpha/(1-\alpha)}\int_{-\infty}^{+\infty} du\, u^{-1/2}(u+\lambda)^{\nu/2} \times \exp[\omega(u - u^{1/2}(u+\lambda)^{-\nu/2})], \tag{60'}$$

where $\omega = (\xi/T)^{1/(1-\alpha)}$ as before, and $\lambda = \mu(\xi/T^{\alpha})^{1/(1-\alpha)}$. In the large ω limit, one can again use the saddle point method. In this instance, however, two distinct cases arise. Namely, the saddle point can be either large or small compared to λ. In the former case ($u_s \gg \lambda$), which corresponds to the "short time regime," one simply recovers the previous results, whereas in the other case ($u_s \ll \lambda$), which corresponds to the "long time" limit, one obtains a normal diffusion regime.

Let us consider first the short time regime ($u_s \gg \lambda$). In this limit, one can forget about the λ term in the expression for f and g. The saddle point is therefore given by the equation already used before, and its value is $u_s = (\alpha)^{1/(1-\alpha)}$. The assumption $u_s \gg \lambda$ implies, that $\xi/t \gg 2/(1-\nu)\mu^{2/(1+\nu)}$. This is the quantitative way of defining the "short time limit."

In the opposite limit, u has to be neglected relative to λ in the equation that defines the saddle point. The saddle point is thus the solution of

$$\frac{d}{du}(u - u^{1/2}\lambda^{-\nu/2})(u = u_s) = 0, \tag{61}$$

which gives $u_s = \frac{1}{4}\lambda^{-\nu}$. In order to be consistent, one has to insist that $u_s \ll \lambda$; that is, $\xi/2T \ll 1 \cdot \mu^{2/(1+\nu)}$. Now, the value of the argument in the exponential at the saddle point is equal to $(\mu^{-\nu})\xi^2/4T$. Last, the second derivative of the argument of the exponential is $2(T^3/\xi^2)$. Again, using standard results about the saddle point method, one obtains

$$f(\xi,T) = \sqrt{(\mu^{\nu}/4\pi T)}\exp(-(\xi^2/4\mu^{\nu}T)), \tag{62}$$

$$g(\xi,T) = (1/\sqrt{4\pi\mu^{\nu}T}) \times \exp(-(\xi^2/4\mu^{\nu}T)). \tag{63}$$

Contrary to the "short time" limit, these functions describe a normal diffusion process, since the size of the invaded region grows like $T^{1/2}$. Indeed, the asymptotic expression for g is nothing but the Green's function for the heat equation, with a diffusion coefficient μ^{ν}. This simple result can be understood if one returns to (54) and considers processes varying on a time scale no faster than unity. In this case, (45) implies that f and g are proportional, and, therefore, they obey an ordinary diffusion equation.

From our analysis so far, the results show that the solution has two distinct behaviors. When $\xi/T \gg \mu^{(\nu+1)/2}$ (small time limit), one expects anomalous diffusion, with the $T^{1/3}$ power law. On the other hand, when $\xi/T \ll \mu^{(\nu+1)/2}$ (large time limit), one recovers normal diffusion. It turns out that the importance of these two regimes depends very much on the time one considers. Indeed, the value of the exponentials in f and g have the common value $\exp(-\mu T)$ when $\xi/T \approx \mu^{(\nu+1)/2}$. Therefore, when $T < \mu^{-1}$, the anomalous law is observable at large values of the space variable ξ, because the functions f and g still have non-negligible values when the transition between the two regimes occurs. On the other hand, the normal diffusion law has little influence, since the exponential decay is unimportant from $\xi = 0$ up to $\xi = T\mu^{(\nu+1)/2}$. In the other case, where $T > \mu^{-1}$, the anomalous diffusion is not observable, because the solution is completely damped before the crossover point is reached. In this case the normal diffusive regime governs the dispersion of tracer, as long as it takes significant values.

V. CONCLUSION

The phenomenon of anomalous diffusion has recently received a great deal of attention. The role of trapping, or very long correlation, has been discussed in detail, in particular in the context of condensed matter physics (disordered materials).[9] In the hydrodynamic case, dispersion in a channel or tube with branching pipes can be shown an example, where trapping leads to an anomalous diffusion, as recently shown by one of us.[7] For stratified porous media, transverse diffusion of particles may lead to very correlated particle motion, and thus to an anomalous diffusion.

The present work offers another example that can be worked out completely, and where anomalous diffusion is expected as a transient regime, before normal diffusion takes over. The ultimate diffusive behavior is already nontrivial, since it involves an effective diffusion coefficient very much enhanced, compared to the molecular diffusivity κ (by a factor $\mathrm{Pe}^{1/2}$). This prediction, resulting from the work of Rosenbluth *et al.*[1] and Shraiman[2] has been recently checked experimentally.[10] The new prediction here is that the number of invaded rolls grows as $t^{1/3}$, for time $t \ll T_d$, the diffusion time. A crossover occurs at a time of order T_d. Preliminary experimental results tend to confirm these predictions.[11]

ACKNOWLEDGMENT

William R. Young was supported by NSF Grant No. 8421074-OCE.

APPENDIX A: DERIVATION OF EQ. (2.7)

We will begin by rewriting (1), using streamfunction φ and arclength l as coordinates. One finds

$$\theta_t + q\theta_l - \kappa[(\nabla\varphi\cdot\nabla\varphi)\theta_{\varphi\varphi} + (2\nabla\varphi\cdot\nabla l)\theta_{l\varphi} + (\nabla l\cdot\nabla l)\theta_{ll} + (\nabla^2\varphi)\theta_\varphi + (\nabla^2 l)\theta_l] = 0, \tag{A1}$$

where $q = \sqrt{u^2+v^2} = |\nabla\varphi|$ is the fluid speed. When the Peclet number is large, (A1) can be simplified to

$$\theta_t + q\theta_l - \kappa(q^2\theta_{\varphi\varphi} + \zeta\theta_\varphi) = 0, \tag{A2}$$

where $\zeta \equiv \nabla^2\varphi$. In fact, in the center of the cell, the second term in (A2) is larger than the others and its dominance implies (13), i.e., at leading order the concentration is uniform around streamlines. At next order, all terms in (A2) appear and (14) is obtained as a solvability condition for this inhomogeneous problem. More details can be found in Rhines and Young,[5] and Fowler.[6]

In the boundary layer at the edge of the cell, the leading-order balance is between the second and third term in (A2). Introduction of the new variable

$$s \equiv \int q\, dl, \tag{A3}$$

simplifies this to

$$\theta_s = \kappa\theta_{\varphi\varphi}. \tag{A4}$$

Now, at $\varphi = 0$, θ is given by (12) and this is a periodic function of l or s. Averaging (A4) with respect to s yields

$$\partial_\varphi^2 \int \theta\, ds = 0, \tag{A5}$$

or

$$\oint \theta q\, dl$$

is constant through the boundary layer. Thus at the outer edge of the layer, where θ is uniform around streamlines,

$$\theta \approx \frac{\oint \chi q\, dl}{\oint q\, dl}, \tag{A6}$$

which is the effective boundary condition for (14) at $\varphi = 0$.

APPENDIX B: LOCAL ANALYSIS OF THE CELL STRUCTURE

In this appendix we calculate the constant Δ in (21a) using a local approximation of the streamfunction. We suppose that this function has the form

$$\varphi = \varphi_{\max}\varphi_*(x_*, y_*), \quad x_* = x/L_x, \quad y_* = y/L_y. \tag{B1}$$

As indicated in Fig. 1, it is easy to expand φ near the boundary. The constants c_1 and c_2 introduced in that figure are dimensionless. It may be helpful to refer to a specific model streamfunction

$$\varphi = \varphi_{\max}\sin\pi x_*(16y_*^2(y_*-1)^2), \tag{B2}$$

for which $c_1 = 16\pi$, $c_2 = 32$, $\zeta_* = \sin\pi x_*$, and $v_* = y_*^2(y_*-1)^2$.

The travel time around an outer streamline is dominated by the horizontal sections near the no-slip boundary. Hence to leading order, when $\varphi \ll \varphi_{\max}$,

$$T(\varphi) \approx \left(\frac{1}{2}c_2\varphi_{\max}\varphi\right)^{-1/2} L_xL_y\int_0^1 \zeta_*^{-1/2}\, dx_*, \tag{B3}$$

and so from (18),

$$a(\varphi) = L_xL_y\left(1 - \int_0^1 \zeta_*^{-1/2}\, dx_*\left(\frac{8\varphi}{c_2\varphi_{\max}}\right)^{1/2} + \cdots\right). \tag{B4}$$

In contrast to the travel time, the circulation around an outer streamline is dominated by the vertical portions of the path, i.e., if $\varphi \ll \varphi_{\max}$,

$$C = \oint q\, dl,$$

$$\approx 2c_1\left(\frac{\varphi_{\max}L_y}{L_x}\right)\int_0^1 v_*\, dy_*, \tag{B5}$$

so that in combining (B3)–(B5), the diffusivity in (19a) is

$$D(a) \approx \Delta(1 - a/A)^{-1},$$

$$\Delta \equiv \left(\frac{8c_1}{c_2}\right)\left(\int_0^1 \zeta_*^{-1/2}\, dx_*\right)^2\left(\int_0^1 v_*\, dy_*\right)\kappa L_y^2. \tag{B6}$$

With the specific model in (B2), the dimensionless constants are easily calculated and one has

$$\Delta = 1.164\kappa L_y^2. \tag{B7}$$

APPENDIX C: CALCULATION OF THE INTERCELLULAR TRANSPORT WHEN L_x/L_y IS OF ORDER 1

In Sec. III we have argued that the effective diffusion coefficient in the case of very elongated rolls ($L_x \gg L_y$) should be given by (34a) and (34b). In this appendix the range of validity of this calculation is examined, and the complementary case, where the aspect ratio of the roll is order 1, is considered.

Let us consider a steady, periodic, two-dimensional flow pattern between rigid walls. The streamfunction φ is periodic in the x direction with a periodicity L_x, and there is no slip at the walls located at $y = 0$ and $y = L_y$. A passive tracer is introduced in the rolls. The dimensionless parameters in this problem are the aspect ratio of the rolls, $\beta = L_x/L_y$, and the Peclet number, $P_e = \varphi_{\max}/\kappa$, where κ is the diffusion coefficient of the tracer we are considering.

We are concerned here with the large Peclet number limit. In Sec. III we have distinguished the case where the aspect ratio β is large. The range of validity of the calculation in Sec. III is examined. We consider a steady solution where a concentration gradient is imposed in the cell. The enhancement of diffusivity results from the boundary layers in between rolls, where transport is enhanced by large (local) concentration gradients. The use of (A4) as a starting point in the calculation leading to the flux expression [(34a)

and (34b)] rests on the hypothesis that the gradients are concentrated in a narrow boundary layer. If the boundary layer width is δ, the flux of tracer between rolls, $-\kappa\int\theta_x\,dy$, is of order $\kappa\theta(L_y/\delta)$. In order to estimate the boundary layer width, a dominant balance argument can be used for the advection–diffusion equation: $u\cdot\nabla\theta=\kappa\nabla^2\theta$. Along the separatrix, the $u\cdot\nabla\theta$ term is of the order of magnitude $v_y\theta/L_y \approx\varphi_{\max}\theta/(L_xL_y)$. The order of magnitude of the diffusive term is given by $\kappa\theta_{\max}(1/\delta^2,1/L_y^2)$. Assuming that $\delta\ll L_y$, we find $\delta\approx L_y(\beta/P_e)^{1/2}$. Therefore the calculation presented in Sec. III requires $\beta\ll P_e$.

The approximation made in the evolution of the flux in (33a) and (33b) is that the horizontal length of the rolls is so large that the tracer is completely mixed during its passage along the wall, before it reaches the separatrix (see Fig. 2). In the other limit, where $\beta\approx 1$, no mixing occurs and the concentration profile remains unchanged as one goes along the horizontal plate. In order to estimate precisely for which aspect ratio the mixing becomes important, we again use dominant balance arguments.

In the limit where a boundary layer builds up along the separatrix, it is a simple matter to evaluate the width of the layer in which concentration gradients are localized right after the turn. If one assumes, as is justified in Rosenbluth *et al.*[1] and Shraiman,[2] that diffusion is not effective during the turn, concentration simply follows the streamlines around the corner. Now, the boundary layer width $\delta=L_y(\beta/P_e)^{1/2}$ right before the turn becomes, after the turn, $\delta_w=L_y(1/\beta P_e)^{1/4}$. This width has to be compared with the layer where diffusion plays a role. Taking into account the no-slip condition at the walls, the advection–diffusion equation takes, along the boundaries $y=0,L_y$, the following simpler form:

$$\varphi_{*x_*}\theta_{y_*}-\varphi_{*y_*}\theta_{x_*}=(\beta/P_e)\theta_{y_*y_*},$$

$$\varphi_*=\tfrac{1}{2}c_2y_*^2\zeta_*(x_*),$$

where the notation in Fig. 1 has been used. A dominant balance in this equation shows that diffusion is important in a thin layer of width $\delta_\kappa=L_y(\beta/P_e)^{1/3}$. Therefore this diffusive layer has a negligibly small width compared to the size of the layer that carries the tracer, when $\delta_\kappa\ll\delta_w$, that is, when $\beta\ll P_e^{1/7}$. When $\beta\gg P_e^{1/7}$, the distance between the walls is so large that mixing makes the tracer concentration profile uniform before it reaches the separatrix, as assumed in Sec. III. In the opposite case, when $\beta\ll P_e^{1/7}$, the layer where molecular diffusion is important is much smaller than the region of fluid that carries tracer.

[1]M. N. Rosenbluth, H. L. Berk, I. Doxas, and W. Horton, Phys. Fluids **30**, 2636 (1987).

[2]B. Shraiman, Phys. Rev. A **36**, 261 (1987).

[3]The boundary layer techniques used to treat advection–diffusion in two-dimensional, spatially periodic, weakly diffusive flows were originally developed in dynamo theory. See A. M. Soward, J. Fluid Mech. **180**, 267 (1987); this is a recent reference that reviews earlier work in this area.

[4]This power law applies only if there is "no slip" at $y=0$ and L_y. In the case of slippery boundaries, the number of cells that are invaded grows as $t^{1/4}$. These power laws are derived using simple scaling arguments by E. Guyon, J. P. Hulin, C. Baudet, and Y. Pomeau, Nucl. Phys. B **2**, 271 (1987), and by Y. Pomeau, A. Pumir, and W. R. Young, C. R. Acad. Sci. (Paris) **306** II, 741 (1988).

[5]P. B. Rhines and W. R. Young, J. Fluid Mech. **133**, 133 (1983).

[6]A. Fowler, Stud. Appl. Math. **72**, 161 (1985).

[7]W. R. Young, J. Fluid Mech. **193**, 129 (1988).

[8]N. G. de Bruijn, *Asymptotic Methods in Analysis* (Dover, New York, 1981).

[9]For a recent reference see, for example, J. P. Bouchaud, A. George, and P. Ledoussal, J. Phys. (Paris) **48**, 1855 (1987) and references therein.

[10]T. H. Solomon and J. P. Gollub, Phys. Fluids **31**, 1372 (1988).

[11]O. Cardoso and P. Tabeling, submitted to Europhys. Lett.